

# Vanishing Higgs potential at the Planck scale in singlets extension of the standard model

Naoyuki Haba<sup>1</sup>, Hiroyuki Ishida<sup>1</sup>, Kunio Kaneta<sup>2</sup>, and Ryo Takahashi<sup>1</sup>

<sup>1</sup>*Graduate School of Science and Engineering, Shimane University,  
Matsue, Shimane 690-8504, Japan*

<sup>2</sup>*ICRR, University of Tokyo, Kashiwa, Chiba 277-8582, Japan*

## Abstract

We discuss the realization of a vanishing Higgs potential at the Planck scale, which is required by the multiple point criticality principle (MPCP), in the standard model with singlet scalar dark matter and a right-handed neutrino. We find the scalar dark matter and the right-handed neutrino play crucial roles for realization of the MPCP, where a neutrino Yukawa becomes effective above Majorana mass of the right-handed neutrino. Once the top mass is fixed, the MPCP at the (reduced) Planck scale and the suitable dark matter relic abundance determine the dark matter mass,  $m_S$ , and Majorana mass of the right-handed neutrino,  $M_R$ , as  $8.5 \text{ (8.0)} \times 10^2 \text{ GeV} \leq m_S \leq 1.4 \text{ (1.2)} \times 10^3 \text{ GeV}$  and  $6.3 \text{ (5.5)} \times 10^{13} \text{ GeV} \leq M_R \leq 1.6 \text{ (1.2)} \times 10^{14} \text{ GeV}$  within current experimental values of the Higgs and top masses. This scenario is consistent with current dark matter direct search experiments, and will be confirmed by future experiments such as LUX with further exposure and/or the XENON1T.

# 1 Introduction

The Higgs particle was discovered at the LHC experiment [1, 2] but one finds no evidence to support the existence of physics beyond the standard model (SM), so far. Thus, a question, “How large is new physics scale?”, is important for the SM and new physics. One simple answer is that the SM is valid up to the Planck scale, i.e. there is no new physics between the electroweak (EW) and the Planck scales. In the case, the current experimental values of the Higgs and top masses might imply a vanishing Higgs potential at the Planck scale. In fact, there are intriguing researches about this possibility. For instance, Ref. [3] proposed the multiple point criticality principle (MPCP). This principle means that there are two degenerate vacua in the SM Higgs potential,  $V(v) = V(M_{\text{pl}}) = 0$  with  $V'(v) = V'(M_{\text{pl}}) = 0$ , where  $V$  is the Higgs potential,  $v$  is the vacuum expectation value (VEV) of the Higgs, and  $M_{\text{pl}}$  is the Planck scale. One is at the EW scale where we live and another is at the Planck scale, which can be realized by the Planck scale boundary conditions (BCs) of the vanishing Higgs self-coupling ( $\lambda(M_{\text{pl}}) = 0$ ) and its  $\beta$ -function ( $\beta_\lambda(M_{\text{pl}}) = 0$ ). As a result, Ref. [3] pointed out that the principle predicts  $135 \pm 9$  GeV Higgs mass and  $173 \pm 5$  GeV top mass, which are close to the experimental values but not the current center values. Furthermore, an asymptotic safety scenario of gravity [4] predicted 126 GeV Higgs mass with a few GeV uncertainty and this scenario also pointed out  $\lambda(M_{\text{pl}}) \simeq 0$  and  $\beta_\lambda(M_{\text{pl}}) \simeq 0$  (see also [5]-[14] for more recent analyses). In this paper, we discuss the realization of a vanishing Higgs potential at the Planck scale, which is required by the MPCP, in the SM with singlet scalar dark matter (DM) and a right-handed neutrino.

An important motivation of the gauge singlets extension of the SM is to explain DM and the tiny active neutrino mass. In this extension, the scalar particle can be DM when it has odd parity under an additional  $Z_2$  symmetry [15] (see also [16]-[26]). The right-handed Majorana neutrino can generate the tiny active neutrino mass via the type-I seesaw mechanism. Once the scalar (right-handed neutrino) is added to the SM, an additional positive (negative) contribution appears in  $\beta_\lambda$ .<sup>1</sup> In addition, since it is difficult to reproduce 126 GeV Higgs mass and  $173.34 \pm 0.76$  GeV top pole mass [33] at the same time under the MPCP at the Planck scale in the SM, it is intriguing to study whether the principle can be realized with the center values of the Higgs and top masses in the singlets extension of the SM, or not.

In this paper, we discuss the realization of the vanishing Higgs potential at the Planck scale, which is required by the MPCP, in the SM with singlet scalar DM and the right-handed neutrino. We find the scalar DM and the right-handed neutrino play crucial roles for the realization of the MPCP, where a neutrino Yukawa becomes effective above Majorana mass of the right-handed neutrino. Once the top mass is fixed, the MPCP at the (reduced) Planck scale and the suitable DM relic abundance determine the DM mass,  $m_S$ , and the Majorana mass of the right-handed neutrino,  $M_R$ , as  $8.5 \text{ (8.0)} \times 10^2 \text{ GeV} \leq m_S \leq 1.4 \text{ (1.2)} \times 10^3 \text{ GeV}$  and

---

<sup>1</sup>See also [18, 23, 24] for researches of the vacuum stability and the coupling perturbativity in the SM with scalar DM, and [27, 28, 29, 30] for explaining the recent BICEP2 result [31] in the framework of the Higgs inflation [32] with gauge singlet fields.

$6.3 (5.5) \times 10^{13} \text{ GeV} \leq M_R \leq 1.6 (1.2) \times 10^{14} \text{ GeV}$  within current experimental values of the Higgs and top masses. This scenario can be consistent with bounds from DM detection experiments, and will be confirmed by future experiments such as LUX with further exposure and/or the XENON1T.

## 2 Singlets extension of the SM

The relevant Lagrangians of the singlets extension of the SM are given by

$$\mathcal{L} = \mathcal{L}_{\text{SM}} + \mathcal{L}_{\text{singlets}}, \quad (1)$$

$$\mathcal{L}_{\text{SM}} \supset -\lambda \left( |H|^2 - \frac{v^2}{2} \right)^2, \quad (2)$$

$$\mathcal{L}_{\text{singlets}} = -\frac{\bar{m}_S^2}{2} S^2 - \frac{k}{2} |H|^2 S^2 - \frac{\lambda_S}{4!} S^4 - \left( \frac{M_R}{2} \bar{N}^c N + y_N \bar{L} \tilde{H} N + c.c. \right) + (\text{kinetic term}), \quad (3)$$

where the SM Lagrangian including the Higgs potential is given by  $\mathcal{L}_{\text{SM}}$ , and  $H$  is the Higgs doublet ( $\tilde{H} \equiv -i\sigma_2 H^*$ ),  $S$  is a gauge singlet real scalar field,  $L$  is the left-handed lepton doublet of the SM,  $N$  is the right-handed neutrino,  $y_N$  is the neutrino Yukawa coupling, and  $M_R$  is the Majorana mass of the right-handed neutrino. In the model, since only the singlet real scalar is assumed to have odd parity under an additional  $Z_2$  symmetry, it can be DM with suitable mass and couplings. The DM mass is given by  $m_S = \sqrt{\bar{m}_S^2 + kv^2/2}$ . The right-handed neutrino generates the small active neutrino mass through the type-I seesaw mechanism.

We utilize the renormalization group equations (RGEs) at 2-loop level in this model, which were firstly given in [30]. Here, we mention the features of RGE runnings of the scalar quartic couplings at the 2-loop level:

- Since the  $\beta$ -function of  $k$  is proportional to  $k$  itself, an evolution of  $k$  is tiny when  $k(M_Z)$  is close to zero. Note that  $k(M_Z) \rightarrow 0$  is the SM limit.
- It is known as the vacuum instability or meta-stability in the SM that  $\lambda(\mu)$  becomes negative within  $\mathcal{O}(10^{10}) \text{ GeV} \lesssim \mu \leq M_{\text{pl}}$  when the experimental center values of the Higgs and top masses are taken. This is induced from the dominant negative contribution of the top Yukawa coupling,  $-6y^4$ . NNLO computations [7] indicate that the  $\lambda(\mu)$  can be positive within  $M_Z \leq \mu \leq M_{\text{pl}}$  for the Higgs mass as  $127 \text{ GeV} \leq m_h \leq 130 \text{ GeV}$  with top mass as  $M_t = 173.1 \pm 0.6 \text{ GeV}$  or  $171.3 \text{ GeV} \leq M_t \leq 171.7 \text{ GeV}$  with  $m_h = 126 \text{ GeV}$  (see also [14]).
- The RGE evolution of  $\lambda$  can be raised by the additional positive term  $+k^2/2$  in the  $\beta$ -function of  $\lambda$ . There is also an negative contribution  $-2y_N^4$  to the  $\beta$ -function of  $\lambda$  from the neutrino Yukawa coupling, which pushes down the RGE evolution of  $\lambda$ . We will investigate whether the MPCP can be realized by considering these two contributions in the model, or not.

### 3 Multiple point criticality principle in singlets extension of the SM

The MPCP requires that there are two degenerate vacua in the Higgs potential. One is at the EW scale where we live and another is at the Planck scale. This principle is described as  $V(v) = V(M_{\text{pl}}) = 0$ . In terms of  $\lambda$  and  $\beta_\lambda$ , this principle is written as

$$\lambda(M_{\text{pl}}) = 0, \quad \beta_\lambda(M_{\text{pl}}) = 0, \quad (4)$$

which are obtained from the stationary condition,  $V'(H) = 0$ . The conditions cannot be realized in the SM within the current experimental ranges of top and Higgs masses, i.e. the MPCP in the SM requires lighter top mass and/or heavier Higgs mass [3]. Thus, we need to consider an extension of the SM anyhow.

We investigate realization of eq. (4) in the singlets extension of the SM by solving the 2-loop level RGEs. The scalar DM (neutrino Yukawa) coupling lifts up (pushes down) the running of  $\lambda$ . Thanks to these two contributions in this extension, the positive contribution from the scalar to  $\beta_\lambda$  can avoid the meta-stable vacuum of the SM with the current experimental values of the top and the Higgs masses. The scalar contribution becomes dominant in  $\beta_\lambda$  at the Planck scale, which can realize  $\lambda(M_{\text{pl}}) > 0$  and  $\beta_\lambda(M_{\text{pl}}) > 0$ . And, a negative contribution from the neutrino Yukawa coupling to  $\beta_\lambda$  above the Majorana mass scale can successfully achieve  $\lambda(M_{\text{pl}}) = 0$  and  $\beta_\lambda(M_{\text{pl}}) = 0$ . This is the essence of the realization of the MPCP in this singlets extension of the SM, and the realization is a non-trivial. For the RGEs, decoupling effects of the scalar and the right-handed neutrino should be taken into account below their mass scales by taking away the relevant couplings of them from the corresponding  $\beta$ -functions. In particular, it is very important that the neutrino Yukawa becomes effective above Majorana mass of the right-handed neutrino. For the neutrino sector, the active neutrino mass is induced from the seesaw mechanism ( $m_\nu = y_N^2 v^2 / (2M_R)$ ) and is taken as  $m_\nu = 0.1$  eV. With the relations, the value of  $y_N(M_Z)$  is given by  $y_N(M_Z) = \sqrt{2m_\nu M_R} / v$ . This is an example that one active neutrino mass is obtained. Other two neutrino masses can also be effective in the RGE analyses, but here we assume that other neutrino Yukawa couplings are small enough to be neglected in the analyses.

Our results are summarized in Fig. 1, where the conditions of  $\lambda = 0$  and  $\beta_\lambda = 0$  are depicted by blue and orange curves, respectively. We analyse the realization of the MPCP at both the Planck  $M_{\text{pl}}$  and the reduced Planck scales  $\tilde{M}_{\text{pl}}$ , which are shown by the dashed and solid curves in all figures, respectively. In the regions above (below) blue and orange solid curves,  $\lambda(M_{\text{pl}}) > 0$  and  $\beta_\lambda(M_{\text{pl}}) > 0$  ( $\lambda(M_{\text{pl}}) < 0$  and  $\beta_\lambda(M_{\text{pl}}) < 0$ ), respectively. These correspondences are the same for the case of the reduced Planck scale. Figures 1 (a)-(d) are the cases of  $(M_t [\text{GeV}], \lambda_S(M_Z)) = (172.6, 10^{-3})$ ,  $(174.1, 10^{-3})$ ,  $(172.6, 0.5)$ , and  $(174.1, 0.5)$ , respectively, with  $\Omega_S h^2 = \Omega_{\text{DM}} h^2 = 0.12$  [34], where  $\Omega_S$  is the density parameter of  $S$ ,  $\Omega_{\text{DM}}$  is for DM, and  $h$  is the Hubble constant. Since  $S$  is DM in the model, the value of  $k(M_Z)$  is determined by  $m_S$  and  $\Omega_S$ . We utilize `micrOMEGAs` [35] to estimate the relic abundance of  $S$ , and take the

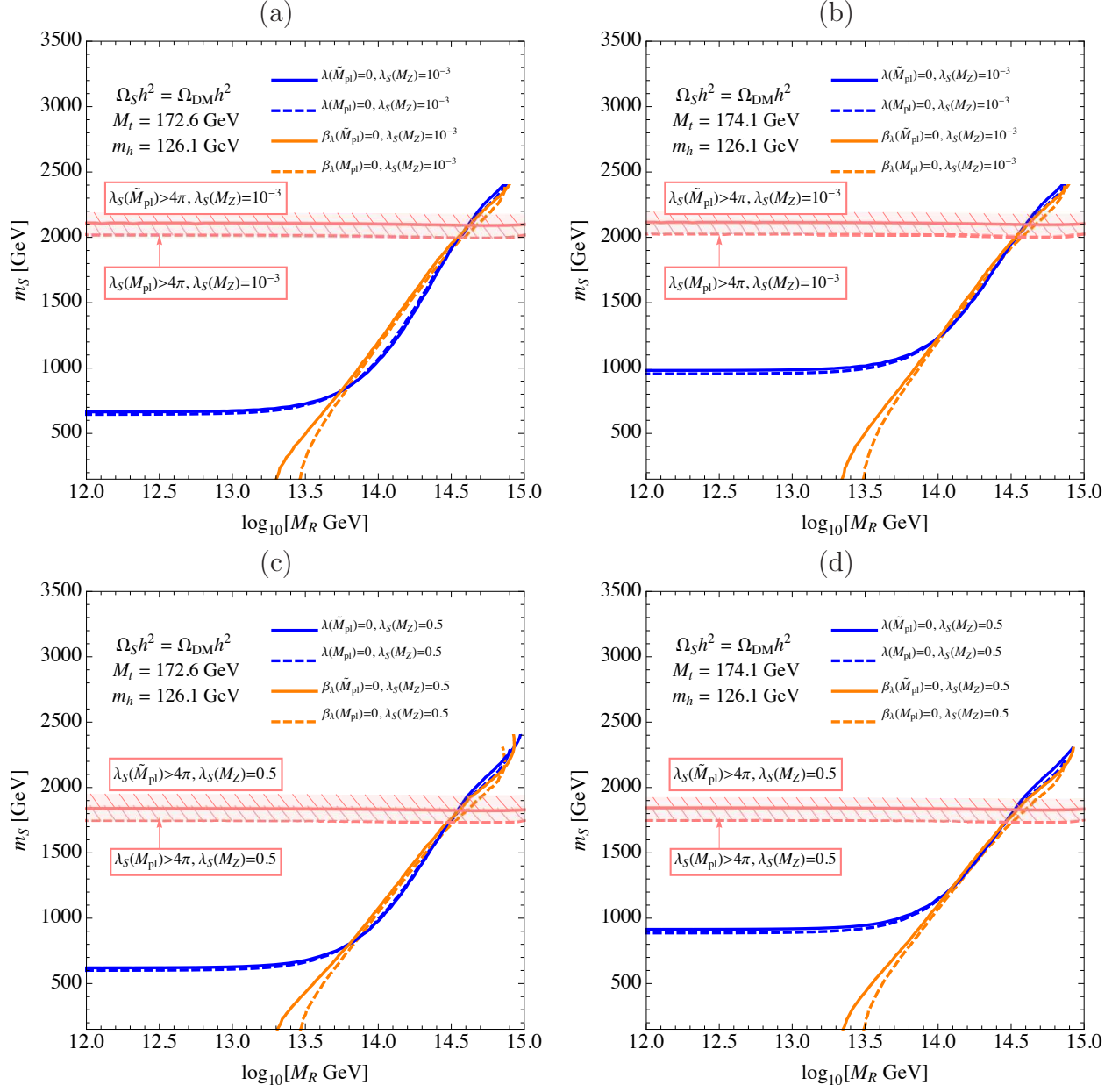


Figure 1: Numerical results for the realization of the MPCP ( $\lambda = 0$  (blue curve) and  $\beta_\lambda = 0$  (orange curve)). The contours for the two conditions at the Planck  $M_{\text{pl}}$  and the reduced Planck  $\tilde{M}_{\text{pl}}$  scales are shown by the dashed and solid curves in all figures, respectively. Figures (a)-(d) correspond to the cases of  $(M_t [\text{GeV}], \lambda_S(M_Z)) = (172.6, 10^{-3})$ ,  $(174.1, 10^{-3})$ ,  $(172.6, 0.5)$ , and  $(174.1, 0.5)$ , respectively.

Higgs mass as 126.1 GeV in the calculation.<sup>2</sup> In the region above the pink dashed and solid lines, self-coupling  $\lambda_S$  exceeds  $4\pi$  at the Planck and reduced Planck scales, respectively, while perturbative calculation is valid in the parameter space below the pink lines. At an intersection point of the blue and orange solid (dashed) curves below the horizontal pink solid (dashed) line, the MPCP can be satisfied within experimentally allowed region of the Higgs, top, and DM masses with suitable scalar quartic couplings up to the (reduced) Planck scale. One can really see that there are some intersection points in Fig. 1. We mention parameter dependences for the realization of the MPCP as follows:

- When  $M_R$  is relatively light as  $M_R < \mathcal{O}(10^{13})$  GeV, the contribution from the neutrino Yukawa coupling to  $\beta_\lambda$  is negligible. Thus, once  $M_t$  is fixed,  $\lambda = 0$  is realized by taking suitable value for only  $m_S$ . This is shown by flat regions of blue curves in the figures. In this region,  $\beta_\lambda(M_{\text{pl}})$  is always positive. A similar case, i.e. the decoupling limit of the right-handed neutrino  $y_N \rightarrow 0$ , was discussed in [24], and our analysis is consistent with the results of [24].
- When  $M_R$  becomes large, we can successfully achieve  $\beta_\lambda(M_{\text{pl}}) = 0$  with  $\lambda(M_{\text{pl}}) = 0$ . The correlation between  $m_S$  and  $M_R$  is seen in slanting regions of the blue curves. One can see that a larger value of  $M_R$  is required to balance with the large scalar contribution.
- Regarding the coupling perturbativity of  $\lambda_S(M_{\text{pl}})$ , it strongly depends on values of  $k(M_Z)$  and  $\lambda_S(M_Z)$  but not on  $M_R$  because the neutrino Yukawa does not contribute to  $\beta_{\lambda_S}$  at 1-loop level. Thus, when one takes a larger  $\lambda_S(M_Z)$ , the bound of the coupling perturbativity of  $\lambda_S(M_{\text{pl}})$  becomes severe for  $m_S$ .
- For heavier  $M_t$ , the MPCP can be realized in heavier  $m_S$ , or equivalent to larger  $k(M_Z)$  (compare Fig. 1 (a) and (b), or (c) and (d)). This is because the dominant negative contribution from the top Yukawa coupling in  $\beta_\lambda$  should be canceled by the positive contribution from  $k$ .
- For larger  $\lambda_S(M_Z)$ , the MPCP is satisfied in lighter  $m_S$  (compare Fig. 1 (a) and (c), or (b) and (d)). Since  $\lambda_S$  coupling gives a positive contribution to the  $\beta$ -function of  $k$ ,  $k$  grows more rapidly for larger  $\lambda_S(M_Z)$ . As a result, smaller  $k(M_Z)$  (or  $m_S$ ) is favored for canceling the negative contribution from the top Yukawa coupling in a larger  $\lambda_S(M_Z)$  case.

Next, Fig. 2 shows the positions of the intersection points in  $(M_R, M_t(\text{or } m_S))$  plane for  $\lambda_S(M_Z) = 10^{-3}$  case.<sup>3</sup> The solid and dashed curves indicate the MPCP solutions at  $\tilde{M}_{\text{pl}}$  and

<sup>2</sup>We also take the strong coupling as  $\alpha_s = 0.1184$ . For the matching terms of  $y_t$  and  $\lambda$  at the top pole mass scale, we take 2-loop results shown in e.g. Refs. [5, 7].

<sup>3</sup>One might also find another intersection point around  $m_S \sim 2.0 \times 10^3$  GeV in each figure  $((m_S [\text{GeV}], M_R [\text{GeV}]) = (1.9 \times 10^3, 3.0 \times 10^{14}), (1.8 \times 10^3, 2.6 \times 10^{14}), (1.6 \times 10^3, 2.5 \times 10^{14}), \text{ and } (1.4 \times 10^3, 1.7 \times 10^{14})$  in Fig. 1 (a), (b), (c), and (d), respectively). Since these points are close to the lines of the coupling perturbativity bound on  $\lambda_S$ , we do not consider these solutions around  $m_S \sim 2.0 \times 10^3$  GeV in this paper anymore. But it could also be the solution for the MPCP.

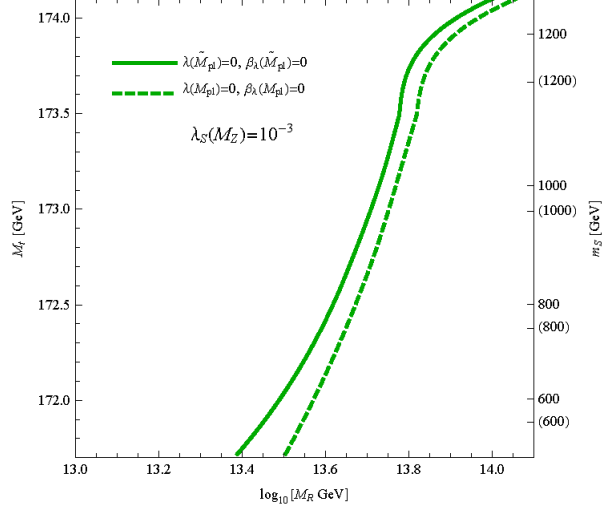


Figure 2: The positions of the intersection points in  $(M_R, M_t(\text{or } m_S))$  plane for  $\lambda_S(M_Z) = 10^{-3}$  case. The solid and dashed curves indicate the MPCP solutions at  $\tilde{M}_{\text{pl}}$  and  $M_{\text{pl}}$ , respectively. The values in the parentheses on the  $m_S$  axis correspond to values in the case of the MPCP at reduced Planck scale while the  $m_S$  values without parentheses are for the case of MPCP at the Planck scale.

$M_{\text{pl}}$ , respectively. We can show that  $m_S$  and  $M_R$  have one to one correspondent ( $m_S$  and  $M_t$  also have one to one correspondent). When one takes larger  $M_t$ , larger  $m_S$  and  $M_R$  are required to achieve  $\lambda = 0$  and  $\beta_\lambda = 0$  at the same time. To summarize, there are seven independent parameters, i.e. five coupling constants ( $\lambda$ ,  $k$ ,  $\lambda_S$ ,  $y$ , and  $y_N$ ) and two mass scales of the singlets ( $m_S$  and  $M_R$ ), in the scalar and Yukawa sectors of the model, in which  $\lambda$  is determined by  $m_h$ . The suitable DM relic abundance relates  $k$  with  $m_S$  and the seesaw mechanism relates  $y_N$  with  $M_R$ . Thus, there are four independent parameters ( $\lambda_S$ ,  $y$ ,  $m_S$ , and  $M_R$ ). When the top mass and  $\lambda_S$  are fixed, the two conditions of the MPCP ( $\lambda = 0$  and  $\beta_\lambda = 0$ ) uniquely determine  $m_S$  and  $M_R$ .<sup>4</sup>

As our result, we find that the MPCP at the (reduced) Planck scale predicts following mass regions,

$$8.5 \text{ (} 8.0 \text{)} \times 10^2 \text{ GeV} \leq m_S \leq 1.4 \text{ (} 1.2 \text{)} \times 10^3 \text{ GeV}, \quad (5)$$

$$6.3 \text{ (} 5.5 \text{)} \times 10^{13} \text{ GeV} \leq M_R \leq 1.6 \text{ (} 1.2 \text{)} \times 10^{14} \text{ GeV}, \quad (6)$$

within  $M_t = (172.6 - 174.1) \text{ GeV}$  and  $10^{-3} \leq \lambda_S(M_Z) \leq 0.5$ . They are obtained by maximal and minimal values of  $m_S$  and  $M_R$  on the intersection points of the two contours of  $\lambda = 0$  and  $\beta_\lambda = 0$  lines which are located at  $(m_S [\text{GeV}], M_R [\text{GeV}]) = (8.6 \text{ (} 8.2 \text{)} \times 10^2, 6.3 \text{ (} 5.5 \text{)} \times 10^{13})$ ,  $(1.3 \text{ (} 1.2 \text{)} \times 10^3, 1.1 \text{ (} 1.0 \text{)} \times 10^{14})$ ,  $(8.5 \text{ (} 8.0 \text{)} \times 10^2, 7.4 \text{ (} 6.3 \text{)} \times 10^{13})$ , and  $(1.4 \text{ (} 1.2 \text{)} \times 10^3, 1.6 \text{ (} 1.2 \text{)} \times$

<sup>4</sup>By extending the model,  $m_S$  and  $M_R$  could be induced dynamically from a dimensional transmutation, which could have a conformal or shift symmetry in the framework of conformal gravity as a UV theory.



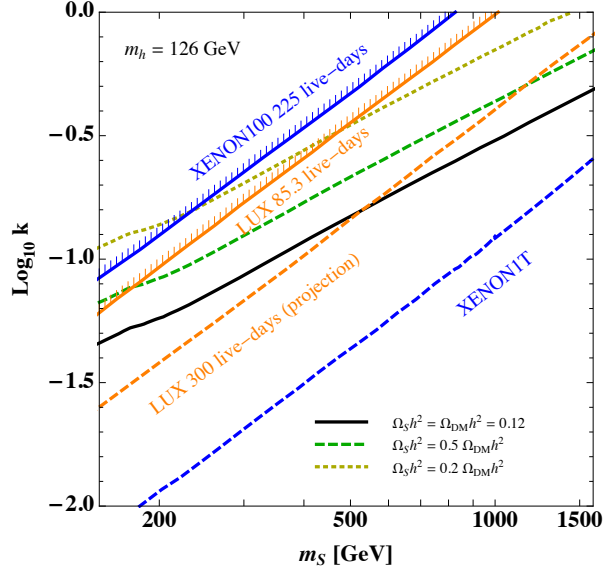


Figure 3: The current experimental bounds on  $m_S$  and  $k$  (XENON100 225 live-days (blue solid line) and LUX 85.3 live-days (orange solid line)), and the future detectability by the LUX 300 day projection (orange dashed line) and the XENON1T (blue dashed line) [36, 37]. The black solid curve indicates the contour of  $\Omega_S h^2 = \Omega_{DM} h^2 = 0.12$ . (The green and yellow dashed curves correspond to  $\Omega_S h^2 = 0.5 \Omega_{DM} h^2$  and  $0.2 \Omega_{DM} h^2$ , respectively.)

$10^{14}$ ) for the case of the MPCP at the (reduced) Planck scale shown in Fig. 1 (a), (b), (c), and (d), respectively.<sup>5</sup>

Finally, we draw Fig. 3, which shows the current experimental bounds on  $m_S$  and  $k$  (XENON100 225 live-days (blue solid line) and LUX 85.3 live-days (orange solid line)) and the future detectability by the LUX (orange dashed line) and the XENON1T (blue dashed line) experiments [36, 37]. The black solid curve indicates the contour of  $\Omega_S h^2 = \Omega_{DM} h^2 = 0.12$ . One can find that the DM mass region eq. (5) for the realization of the MPCP can be consistent with the current DM direct detection experiments and it will be confirmed by future DM direct searches, e.g. the future XENON1T experiment.

## 4 Summary and discussions

We have discussed the realization of the vanishing Higgs potential at the Planck scale, which is required by the MPCP, in the SM with the singlet scalar DM and the right-handed neutrino. We have found the scalar DM and the right-handed neutrino play crucial roles for realization of the MPCP, where the neutrino Yukawa becomes effective above Majorana mass of the right-

<sup>5</sup>There are also intersection points around  $m_S \sim 2.0 \times 10^3$  GeV in the reduced Planck case as  $(m_S [\text{GeV}], M_R [\text{GeV}]) = (2.1 \times 10^3, 3.9 \times 10^{14})$ ,  $(2.0 \times 10^3, 3.5 \times 10^{14})$ ,  $(1.8 \times 10^3, 3.3 \times 10^{14})$ , and  $(1.7 \times 10^3, 2.8 \times 10^{14})$  in Fig. 1 (a), (b), (c), and (d), respectively.



handed neutrino. Once the top mass is fixed, the MPCP at the (reduced) Planck scale and the suitable DM relic abundance determine the DM mass and Majorana mass of the right-handed neutrino as  $8.5 \text{ (} 8.0 \text{)} \times 10^2 \text{ GeV} \leq m_S \leq 1.4 \text{ (} 1.2 \text{)} \times 10^3 \text{ GeV}$  and  $6.3 \text{ (} 5.5 \text{)} \times 10^{13} \text{ GeV} \leq M_R \leq 1.6 \text{ (} 1.2 \text{)} \times 10^{14} \text{ GeV}$  within current experimental values of the Higgs and top masses. The  $m_S$  region is allowed by the current experimental results of the DM direct searches. Moreover, it is of importance that this scenario is testable by the future direct search experiments such as the LUX with further exposure and/or the XENON1T.

Finally, we also show other solutions of the MPCP as examples of different share of  $\Omega_S$  for  $\Omega_{\text{DM}}$ , i.e.  $\Omega_S/\Omega_{\text{DM}} = 0.5$  shown in Fig. 4 (a)-(d) and 0.2 in Fig 4 (e)-(h). The meaning of the lines and colors are the same as in Fig. 1. One can see that the MPCP can be realized in a lighter  $m_S$  region compared to  $\Omega_S/\Omega_{\text{DM}} = 1$  case. At the same time the bound from the coupling perturbativity of  $\lambda_S$  on  $m_S$  becomes more severe when the value of  $\Omega_S/\Omega_{\text{DM}}$  becomes smaller than unity (see Figs. 1 and 4). These are because a smaller  $\Omega_S$  needs larger value of  $k(M_Z)$  for the same DM mass (e.g. see the green ( $\Omega_S/\Omega_{\text{DM}} = 0.5$ ) and the yellow ( $\Omega_S/\Omega_{\text{DM}} = 0.2$ ) dashed curves in Fig. 3). Thus, lighter  $m_S$  gives a solution for the MPCP, and heavier  $m_S$  region is constrained by the coupling perturbativity of  $\lambda_S$  in a smaller  $\Omega_S/\Omega_{\text{DM}}$  case. We also show excluded (shaded) regions of  $m_S < 480 \text{ GeV}$  by the LUX 85.3 live-day WIMP search [36] in Fig. 4 (e)-(h). Regarding with an experimental bound on DM, although there are intersection points around  $m_S \sim 400 \text{ GeV}$  in the case of  $\Omega_S/\Omega_{\text{DM}} = 0.2$  with  $M_t = 172.6 \text{ GeV}$  (see Fig. 4 (e) and (g)), the LUX experiment has ruled out  $m_S < 480 \text{ GeV}$ . As a result, the MPCP is satisfied in regions of  $5.5 \times 10^2 \text{ GeV} \leq m_S \leq 8.4 \times 10^2 \text{ GeV}$  and  $6.3 \times 10^{13} \text{ GeV} \leq M_R \leq 1.6 \times 10^{14} \text{ GeV}$  for  $\Omega_S/\Omega_{\text{DM}} = 0.5$  within  $M_t = (172.6 - 174.1) \text{ GeV}$ , and  $m_S = 5.1 \times 10^2 \text{ GeV}$  and  $M_R = 1.0 \times 10^{14} \text{ GeV}$  for  $\Omega_S/\Omega_{\text{DM}} = 0.2$  with  $M_t = 174.1 \text{ GeV}$ . One can find that these  $m_S$  regions for the realization of the MPCP can also be consistent with the current DM direct detection experiments and it will be confirmed by future DM direct searches.

## Acknowledgement

This work is partially supported by Scientific Grant by Ministry of Education and Science, No. 24540272. The work of R.T. are supported by Research Fellowships of the Japan Society for the Promotion of Science for Young Scientists.

## References

- [1] G. Aad *et al.* [ATLAS Collaboration], Phys. Lett. B **716** (2012) 1 [arXiv:1207.7214 [hep-ex]].
- [2] S. Chatrchyan *et al.* [CMS Collaboration], arXiv:1303.4571 [hep-ex].
- [3] C. D. Froggatt and H. B. Nielsen, Phys. Lett. B **368** (1996) 96 [hep-ph/9511371].
- [4] M. Shaposhnikov and C. Wetterich, Phys. Lett. B **683** (2010) 196 [arXiv:0912.0208 [hep-th]].

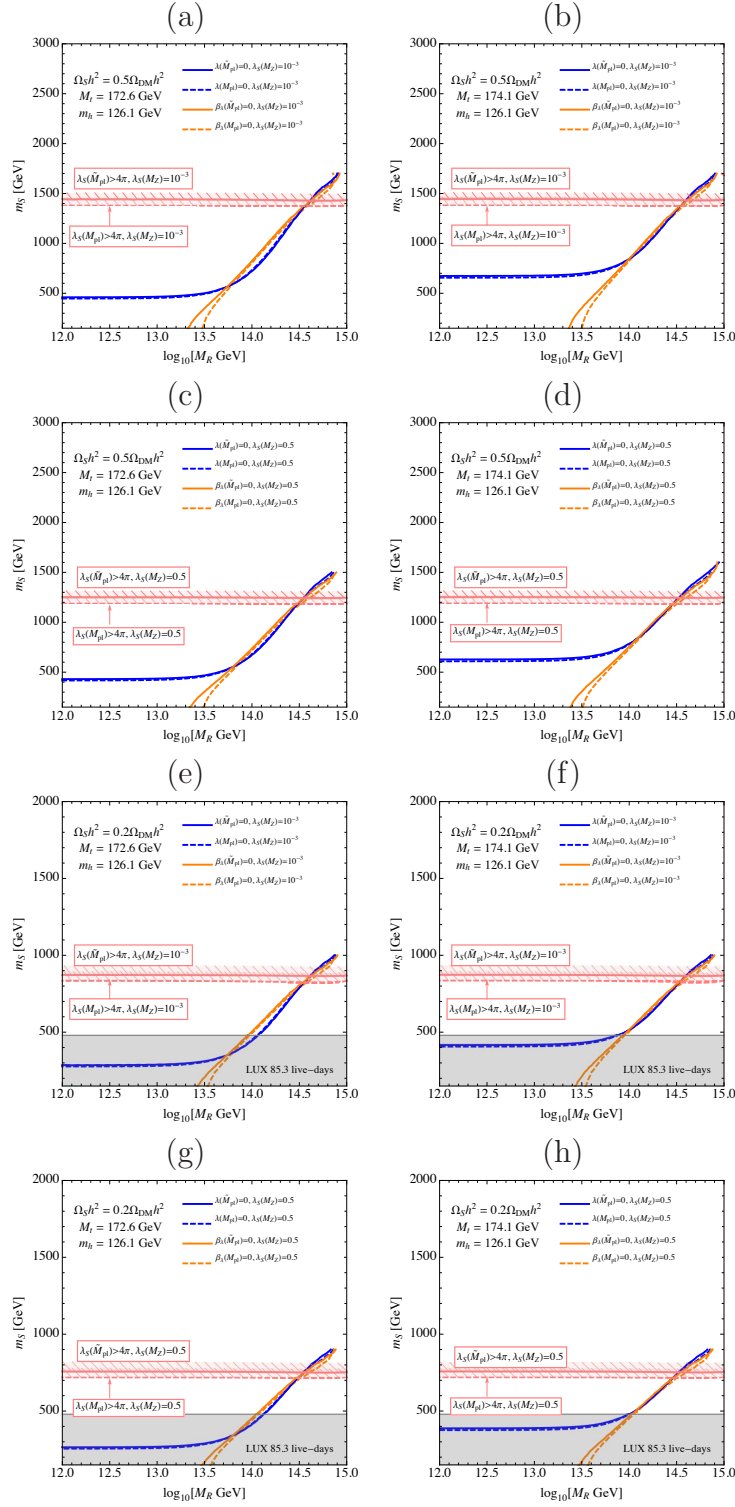


Figure 4: Numerical results for the realization of the MPCP ( $\lambda = 0$  (blue curve) and  $\beta_\lambda = 0$  (orange curve)) in the cases of  $\Omega_S/\Omega_{DM} = 0.5$  ((a)-(d)) and  $\Omega_S/\Omega_{DM} = 0.2$  ((e)-(h)). The meanings of the figures are the same as in Fig. 1.

- [5] M. Holthausen, K. S. Lim and M. Lindner, JHEP **1202** (2012) 037 [arXiv:1112.2415 [hep-ph]].
- [6] F. Bezrukov, M. Y. Kalmykov, B. A. Kniehl and M. Shaposhnikov, JHEP **1210** (2012) 140 [arXiv:1205.2893 [hep-ph]].
- [7] G. Degrandi, S. Di Vita, J. Elias-Miro, J. R. Espinosa, G. F. Giudice, G. Isidori and A. Strumia, JHEP **1208** (2012) 098 [arXiv:1205.6497 [hep-ph]].
- [8] S. Alekhin, A. Djouadi and S. Moch, Phys. Lett. B **716** (2012) 214 [arXiv:1207.0980 [hep-ph]].
- [9] I. Masina, Phys. Rev. D **87** (2013) 053001 [arXiv:1209.0393 [hep-ph]].
- [10] Y. Hamada, H. Kawai and K. -y. Oda, Phys. Rev. D **87** (2013) 053009 [arXiv:1210.2538 [hep-ph]].
- [11] F. Jegerlehner, arXiv:1304.7813 [hep-ph].
- [12] D. Buttazzo, G. Degrandi, P. P. Giardino, G. F. Giudice, F. Sala, A. Salvio and A. Strumia, arXiv:1307.3536 [hep-ph].
- [13] I. Masina and M. Quiros, Phys. Rev. D **88** (2013) 093003 [arXiv:1308.1242 [hep-ph]].
- [14] A. Spencer-Smith, arXiv:1405.1975 [hep-ph].
- [15] V. Silveira and A. Zee, Phys. Lett. B **161** (1985) 136.
- [16] J. McDonald, Phys. Rev. D **50** (1994) 3637 [hep-ph/0702143 [hep-ph]].
- [17] C. P. Burgess, M. Pospelov and T. ter Veldhuis, Nucl. Phys. B **619** (2001) 709 [hep-ph/0011335].
- [18] H. Davoudiasl, R. Kitano, T. Li and H. Murayama, Phys. Lett. B **609** (2005) 117 [hep-ph/0405097].
- [19] B. Grzadkowski and J. Wudka, Phys. Rev. Lett. **103** (2009) 091802 [arXiv:0902.0628 [hep-ph]]; Acta Phys. Polon. B **40** (2009) 3007 [arXiv:0910.4829 [hep-ph]].
- [20] A. Drozd, B. Grzadkowski and J. Wudka, JHEP **1204** (2012) 006 [arXiv:1112.2582 [hep-ph]].
- [21] M. Kadastik, K. Kannike, A. Racioppi and M. Raidal, JHEP **1205** (2012) 061 [arXiv:1112.3647 [hep-ph]].
- [22] S. Baek, P. Ko and W. -I. Park, JHEP **1307** (2013) 013 [arXiv:1303.4280 [hep-ph]].

- [23] N. Haba, K. Kaneta, and R. Takahashi, arXiv:1309.1231 [hep-ph]; Eur. Phys. J. C **74** (2014) 2696 [arXiv:1309.3254 [hep-ph]].
- [24] N. Haba, K. Kaneta, and R. Takahashi, JHEP **1404** (2014) 029 [arXiv:1312.2089 [hep-ph]].
- [25] E. Gabrielli, M. Heikinheimo, K. Kannike, A. Racioppi, M. Raidal and C. Spethmann, Phys. Rev. D **89** (2014) 015017 [arXiv:1309.6632 [hep-ph]].
- [26] S. M. Boucenna, S. Morisi, Q. Shafi and J. W. F. Valle, arXiv:1404.3198 [hep-ph].
- [27] N. Haba and R. Takahashi, arXiv:1404.4737 [hep-ph].
- [28] Y. Hamada, H. Kawai and K. -y. Oda, arXiv:1404.6141 [hep-ph].
- [29] P. Ko and W. -I. Park, arXiv:1405.1635 [hep-ph].
- [30] N. Haba, H. Ishida and R. Takahashi, arXiv:1405.5738 [hep-ph].
- [31] P. A. R. Ade *et al.* [BICEP2 Collaboration], arXiv:1403.3985 [astro-ph.CO].
- [32] F. L. Bezrukov and M. Shaposhnikov, Phys. Lett. B **659** (2008) 703 [arXiv:0710.3755 [hep-th]].
- [33] [ATLAS and CDF and CMS and D0 Collaborations], arXiv:1403.4427 [hep-ex].
- [34] P. A. R. Ade *et al.* [Planck Collaboration], arXiv:1303.5076 [astro-ph.CO].
- [35] G. Belanger, F. Boudjema, A. Pukhov and A. Semenov, Comput. Phys. Commun. **185** (2014) 960 [arXiv:1305.0237 [hep-ph]].
- [36] C. Faham [ for the LUX Collaboration], arXiv:1405.5906 [hep-ex].
- [37] J. M. Cline, K. Kainulainen, P. Scott and C. Weniger, Phys. Rev. D **88** (2013) 055025 [arXiv:1306.4710 [hep-ph]].